Available online at www.sciencedirect.com

SCIENCE DIRECT®

Applied Clay Science 33 (2006) 35 – 42

www.elsevier.com/locate/clay

A hydrogen peroxide sensor based on colloidal MnO_2/Na-montmorillonite

Shaojun Yao [a,b], Shuai Yuan [a], Junhui Xu [a], Ying wang [a], Jianlin Luo [a], Shengshui Hu [a,b,*]

[a] *College of Chemistry and Molecular Sciences, Wuhan University, Wuhan 430072, China*
[b] *State Key Laboratory of Transducer Technology, Chinese Academy of Sciences, Beijing 100084, China*

Received 7 September 2005; received in revised form 27 February 2006; accepted 6 March 2006
Available online 2 May 2006

Abstract

A novel amperometric sensor for the determination of hydrogen peroxide was prepared based on the enhanced oxidation of H_2O_2 at a glassy carbon electrode modified with colloidal MnO_2–Na-montmorillonite (nano-MnO_2/Na-Mont/GCE). The montmorillonite has been devised to support and dispense the MnO_2 nanoparticles. Scanning electron microscopy images (SEM) showed that the MnO_2 nanoparticles were homogeneously dispersed in the colloidal Na-montmorillonite. This colloidal dispersion was dried to form a uniform film when added to the surface of GCE. The voltammetric results showed that MnO_2 nanoparticles could effectively catalyze the oxidation of H_2O_2. The dependence of the response current on H_2O_2 concentration was explored under optimal conditions, and an excellent linear relationship was obtained in the range from 5×10^{-7} to 7.5×10^{-3} M with a minimum detectable concentration of 1.5×10^{-7} M. This sensor has been applied to measure trace concentration of hydrogen peroxide in samples of hair dye.

Keywords: Clay minerals; Sodium montmorillonite; Hydrogen peroxide sensor; MnO_2 nanoparticles

1. Introduction

There has been a significant growth in the application area of mechanically and chemically stable and also fairly inexpensive clay minerals (Van Olphen, 1977). The use of montmorillonite as catalyst supports to construct chemical sensors has gained much attention (Pinnavaia, 1983; Kamat, 1984). A novel hydrogen peroxide sensor was devised by coating the electrode with MnO_2 nanoparticles encaged by colloidal Na-montmorillonite.

Hydrogen peroxide is an intermediate or a product in biochemical reactions catalyzed by oxidase. Thus, the monitoring of H_2O_2 with a reliable, rapid and economic method is of great significance (Klemens et al., 1997). One common approach involves measuring the current when H_2O_2 is oxidized at a solid electrode. A number of studies have been carried out to improve the electrochemical response to H_2O_2 by coating the electrode surface with substances that have catalytic (mediating) activity. These substances can be divided into three

---

* Corresponding author. College of Chemistry and Molecular Sciences, Wuhan University, Wuhan 430072, China. Tel.: +86 27 87218904; fax: +86 27 6875 4067.
E-mail address: sshu@whu.edu.cn (S. Hu).

0169-1317/$ - see front matter © 2006 Elsevier B.V. All rights reserved.
doi:10.1016/j.clay.2006.03.006

groups: (I) Immobilization of transition metal ions, their oxides or complexes on the surface of carbon paste electrode (CPE) or glassy carbon electrode (GCE) (Rice et al., 1983; Oyama and Anson, 1986; Cox and Jaworski, 1989; Wang et al., 1992; Gao et al., 1992; Mannino et al., 1993; Cai et al., 1995; Klemens et al., 1997); (II) Prussian Blue modified or iron phthalocyanine modified electrodes (Itaya et al., 1984; Boyer et al., 1990; Chi and Dong, 1995; Karyakin et al., 1995, 1996, 1999, 2000); and (III) enzymes, tissues and cells modified on CPE (Deng and Dong, 1994; Oungpipat et al., 1995; Razola et al., 2002; Lei et al., 2003, 2004). For the past decades, manganese dioxide (MnO_2) has been proven to be a suitable mediating or catalytic substance to lower the overpotential for H_2O_2 oxidation. J. Wang et al. prepared a GCE with a film of MnO_2 deposited from $MnCl_2$/NaOH solution and showed that it could be used in strongly alkaline solution (Taha and Wang, 1991). Schachl's research group achieved a detection limit of 1.3×10^{-6} M for H_2O_2 using a CPE modified by bulk MnO_2 power (Klemens et al., 1997). In further research they covered the electrode with a layer of glucose oxidase and measured glucose in beer and wine (Emir et al., 2001, 2005).

In this paper, the GCE was modified with MnO_2 nanoparticles. We have shown that nano-MnO_2 has special physical and chemical properties different from common MnO_2 powders (Yao et al., 2006). The common MnO_2 powder is hard to disperse in aqueous solutions. However, MnO_2 nanoparticles can be homogeneously dispersed in colloidal Na-montmorillonite dispersions. It is possible to intercalate MnO_2 nanoparticles into highly swollen Na-montmorillonite (Enea and Bard, 1986; Yoneyama et al., 1989; Dekany et al., 1995). Size-quantized cadmium sulfide semiconductor particles were generated in situ between the interlayer spaces of octadecyl alkylammonium and hexadecyl pyridinium montmorillonites (Kotov et al., 1992). Four years later, Joo's group explored the transport properties of the electroactive $Fe(CN)_6^{3-}$ and $Ru(NH)_3^{3+}$ probe ions through clay films containing CdS nanoparticles. They observed that when a CdS nanoparticle containing montmorillonite was used, the current increased. During the cyclic voltammetry, the limited step is the diffusion through the interlayer region, which is controlled by the porosity. The microencagement and dimensions of nanoparticles depend on the pore structure of the montmorillonite matrix (Fitch and Du, 1991, 1993, 1995; Joo et al., 1996).

A further step was moved towards the application of chemical sensor taking advantage of this property of montmorillonite. Experimental results demonstrated that MnO_2/Na-Mont films enhanced the catalytic activity of MnO_2. The colloidal Na-montmorillonite formed stable and uniform films when coated onto the surface of a GCE. These films are more permeable and conductive than Nafion films, which are commonly used to modify electrodes. The montmorillonite films have large specific surface areas, which enhance the catalytic activity of MnO_2 with H_2O_2. Na-montmorillonite is an inexpensive and inert material. Thus, the colloidal dispersion of MnO_2 nanoparticles in Na-montmorillonite is an excellent material to modify electrodes.

To our knowledge, no work on the modification of GCE by nano-MnO_2 and Na-montmorillonite for H_2O_2 detection has been reported previously. Compared with the other methods of monitoring H_2O_2, the MnO_2/Na-Mont films are excellent electrocatalytic materials for the oxidation of hydrogen peroxide. The response current is linear from 5×10^{-7} to 7.5×10^{-3} M with a detection limit of 1.5×10^{-7} M (S/N=3) achieving a much higher sensitivity than the previous electrode modified by bulk MnO_2 at neutral pH (Klemens et al., 1997).

2. Experimental

2.1. Reagents

Nano-size manganese dioxide (obtained from the Chemistry Department of Wuhan University, China) was synthesized by rheological phase reaction (Yuan et al., 2003). TEM image showed that the particle size of the sample is about 5–50 nm. Na-montmorillonite (SWy-2) was obtained from Missouri University. The cation exchange capacity (CEC) of the clay was 67 meq/100 g (Kuriana et al., 2005). Sodium hexametaphosphate (SPH) was purchased from Shanghai chemical agent Co. Phosphate buffer was prepared by mixing aqueous solutions (0.1 M) of sodium dihydrogenphosphate and di-sodium hydrogenphosphate (Shanghai chemical agent Co.) to achieve the desired pH. Hydrogen peroxide (30%) (Shanghai chemical agent Co.) was standardized by $KMnO_4$ titration. Stock standard H_2O_2 solution containing 100 mM H_2O_2 was prepared freshly each day. Amino acid, ascorbic acid, dopamine, uric acid, adrenaline, caffeine, riboflavin, barbitone, NaCl, $NaNO_3$, Na_2SO_4, $K_3Fe(CN)_6$, oxammonium hydrochloride and other chemicals were analytical reagents. All the chemicals were used without further purification. Water was double distilled.

2.2. Apparatus

Cyclic voltammetry (CV) and amperometry were carried out on a CHI830 electrochemical analyzer (Shanghai Chenhua

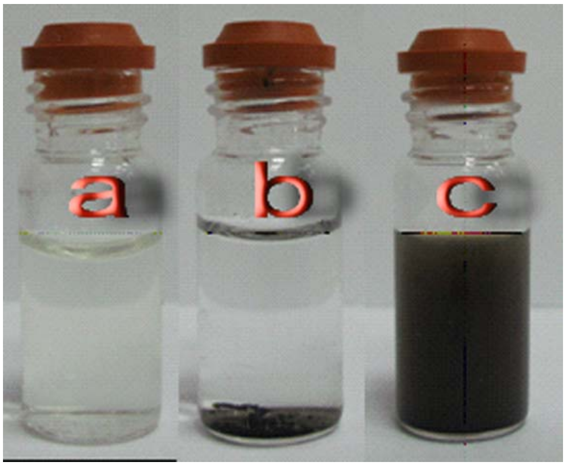

Fig. 1. Photographs of different dispersions: (a) colloidal Na-montmorillonite dispersion; (b) MnO_2 particles in water after ultrasonication for 2 h and resting for 2 h; (c) colloidal dispersion of MnO_2 nanoparticles and Na-montmorillonite after ultrasonication for 2 h and resting for 20 days.

Co., China). The working electrode is a modified glassy carbon electrode with a geometric area of 0.0765 cm^2. The saturated calomel electrode (SCE) is used as reference electrode, and a Pt wire is used as auxiliary electrode. All the potentials were reported versus SCE. Scanning electron microscopy images (SEM) were obtained using a Hitachi X-650 microscope (Japan).

2.3. Preparation of the H_2O_2 sensor

30 mg Na-montmorillonite were added to 2 mL water. After 12 h continuous stirring, the stirrer was turned off and the dispersion was allowed to stand for 5 min. After centrifuging at 9000 rotations per min for 15 min, the supernatant was removed for further use. After that, 1 mg MnO_2 was dispersed into 1 mL of the supernatant with the aid of ultrasonic agitation. During the agitation 0.1% sodium hexametaphosphate was added in some experiments. After 2 h agitation, we obtained a homogeneous, black-brown dispersion of MnO_2–Na-montmorillonite. Before modification, a GCE was polished with a 0.05 μm aluminum slurry (CH Instruments, USA), then rinsed thoroughly with water and finally sonicated in 1:1 HNO_3–H_2O (V/V) and water, each for 1 min. After that, 5 μL of the above-described MnO_2/Na-Mont dispersion was pipetted onto the surface of GCE and the solvent was evaporated at room temperature. By this means, MnO_2/Na-Mont film was physically bound to the electrode surface.

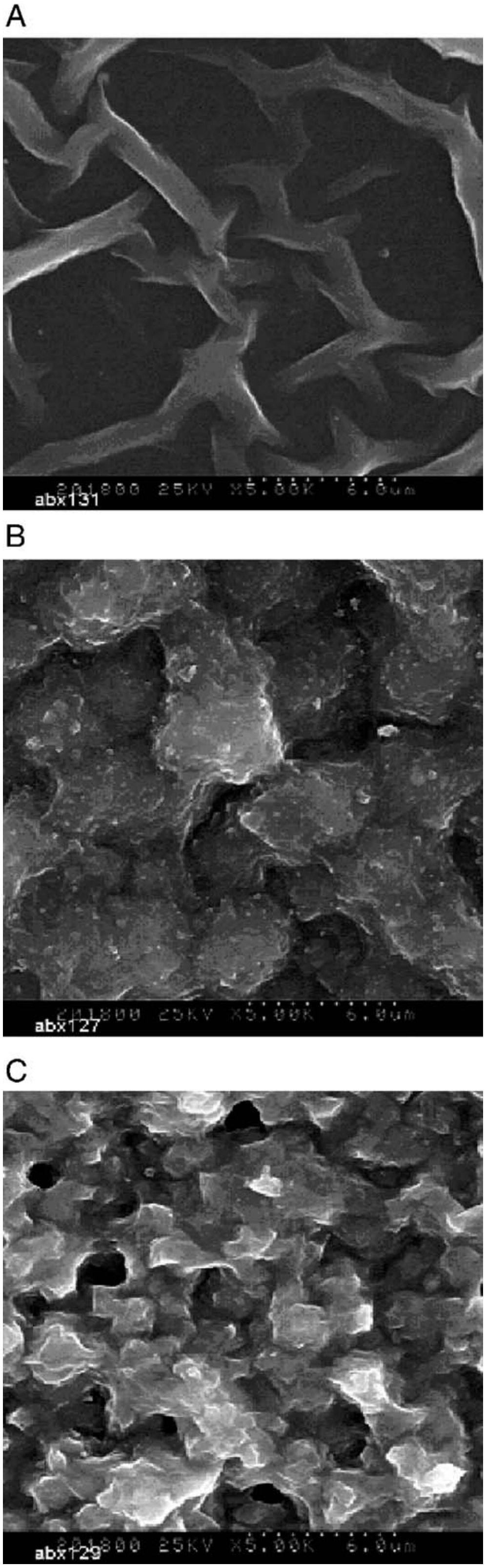

Fig. 2. SEM images of the film on the surface on the glassy carbon electrodes. (A) SEM image of the Na-montmorillonite film on GCE. (B) SEM image of MnO_2 particles and Na-montmorillonite on GCE (without $(NaPO_3)_6$). (C) SEM image of MnO_2 particles and Na-montmorillonite on GCE (with $(NaPO_3)_6$).

The Na-montmorillonite coated electrode was prepared by the same procedure explained above without MnO_2.

2.4. Amperometric measurement of H_2O_2

Amperometry was carried out in an electrochemical cell holding 10 ml of 0.1 M phosphate buffer (pH = 7.4). Magnetic stirring provided the convective transport in the amperometric experiment. A holding potential of 0.65 V was applied to the modified electrode. The background current was allowed to decay to a constant value before H_2O_2 solution was added to the cell. The current–time curves for the amperometric experiments were all recorded at 25 ± 0.5 °C. The calibration curve was obtained by amperometric responses when added the same amount of H_2O_2 standard solution into cell.

3. Results and discussion

The colloidal Na-montmorillonite dispersion is transparent and colorless (Fig. 1a). MnO_2 nanoparticles are insoluble in water (Fig. 1b). In the presence of montmorillonite, MnO_2 nanoparticles formed a dispersion that is stable for more than two weeks (Fig. 1c). The SEM image of Na-montmorillonite showed a loose and reticulate appearance on the surface of GCE. Fig. 2B shows that the MnO_2 nanoparticles are enwrapped by Na-montmorillonite. A more uniform distribution is obtained with the aid of $(NaPO_3)_6$, and there are numerous cavities that facilitated the penetration of H_2O_2 (Fig. 2C).

The film containing $(NaPO_3)_6$ is not so fragile as without $(NaPO_3)_6$. $(NaPO_3)_6$ can negatively charge the surface of nanoparticles which strengthens the electrostatic repulsion (Song et al., 2005). Apparently this interaction makes the film more flexible.

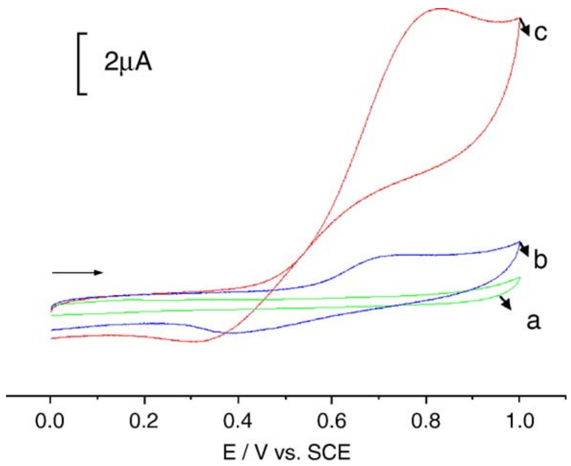

Fig. 3. Cyclic voltammograms of H_2O_2 on MnO_2/montmorillonite/GCE (containing $(SPH)_6$) in phosphate buffer (pH = 7.4); scan rate: 50 mV/s. (Curve a) Bare GCE with 1 mM H_2O_2. (Curve b) MnO_2/Na-montmorillonite/GCE without H_2O_2. (Curve c) as b in the presence of 1 mM H_2O_2.

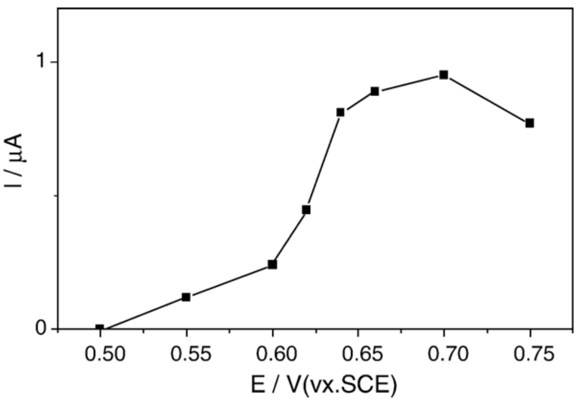

Fig. 4. Effect of applied potential on the amperometric response of 0.5 mM H_2O_2 in phosphate buffer solution (pH = 7.4).

During shrinking by vaporization of the water the encagement becomes more compact. Even when such a film is placed into water or an aqueous electrolyte solution, the Na-montmorillonite still supports the nanoparticles and small molecules (including H_2O_2) can penetrate into the film. This is one of the major reasons why such a film greatly enhances the catalytic effect of MnO_2 nanoparticles.

Fig. 3 shows the cyclic voltammograms (CV) for hydrogen peroxide with the prepared electrodes. With bare GCE and Na-montmorillonite/GCE, no oxidation peak was observed within the applied potential range for 1 mM H_2O_2 in PB solution (curve a). In the absence of hydrogen peroxide, there is a pair of broad but weak waves between 0.2 and 0.8 V (curve b). It may be assigned to the reduction of MnO_2 to Mn(II,III) and the

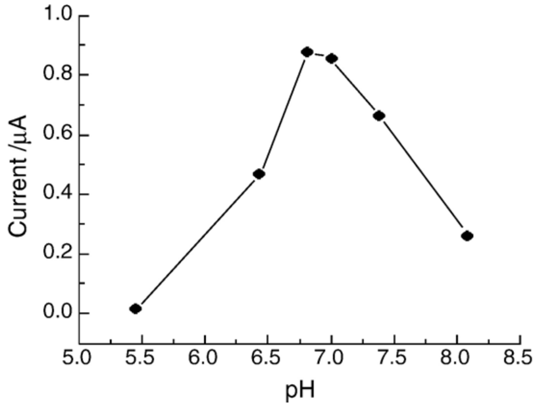

Fig. 5. Effect of solution pH value on the amperometric response of 0.5 mM H_2O_2 in phosphate buffer (pH 7.4). Applied potential: 0.65 V.

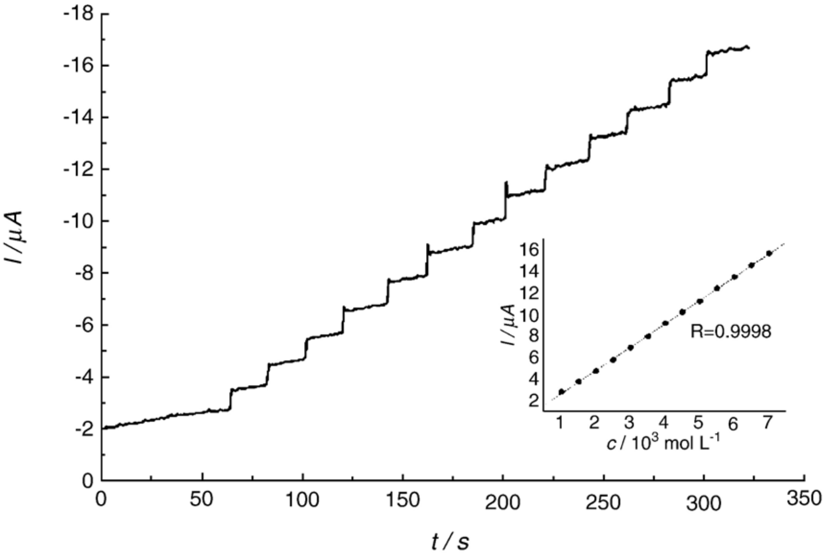

Fig. 6. Dynamic responses of MnO_2/Na-montmorillonite/GCE (with $(NaPO_3)_6$) to successive addition of 0.5 M H_2O_2 at pH = 7.4. Applied potential 0.65 V. Sub-figure: Calibration curve of H_2O_2 amperometric biosensor based on MnO_2/Na-montmorillonite/GCE (with $(NaPO_3)_6$) in phosphate buffer (0.1 M, pH = 7.4). Applied potential 0.65 V.

reoxidation of Mn(II,III) back to MnO_2 (Emir et al., 2001; Yin et al., 2001: Samo et al., 2004). In the presence of H_2O_2, the cyclic voltammogram displays a sensitive oxidative peak at around 0.7 V (curve c). The current for oxidation of Mn(II,III) to MnO_2 significantly increases with increasing H_2O_2 concentration. The characteristic shape of the cyclic voltammogram in this potential region indicates that the signal is probably due to a parallel catalytic reaction. As soon as MnO_2 is reduced to lower states by H_2O_2, it is electro-oxidized back to MnO_2 at the electrode surface (Emir et al., 2001):

$$MnO_2 + H_2O_2 \rightarrow MnO(\text{or } Mn_2O_3) + H_2O$$

$$MnO(\text{or } Mn_2O_3) + 2e \rightarrow MnO_2$$

Since the above two reactions are fast, the parallel current is much higher than the oxidation current of MnO_2 on the electrode surface without H_2O_2.

The applied constant potential for amperometry at the working electrode was chosen on the basis of the electrochemical behavior of nano-MnO_2 (Fig. 3). The optimization is demonstrated in Fig. 4, where the signal height for 1 mM hydrogen peroxide is plotted against the operating potential. Although at 0.70 V where the signal is highest, we choose 0.65 V as the operating potential because above 0.65 V there is increased noise, which is a disadvantage for measuring low H_2O_2 concentrations.

The ratio between MnO_2 and Na-montmorillonite in the film is a very important parameter for optimal sensor operation, because the catalytical current depends not only on the concentration of H_2O_2 but also on the concentration of activated MnO_2 in the film. Sensitivity

Table 1
Relative changes in the current response of H_2O_2 in the presence of interferents

Groups	Interferent	Changes in current (%)		
		Conc. (0.1 mM)	0.5 mM	1 mM
1	NaCl	0	0	0
	$NaNO_3$	0	0	0
	$NaSO_4$	0	0	0
	$K_3Fe(CN)_6$	0	<5	<5
2	Gly	0	−13	−30
	Arg	0	−15	−33
	Glu	0	−11	−25
	NaGlu	0	−15	−37
	Asn	0	−19	−35
3	Ascorbic acid	17	58	230
	Uric acid	9	14	106
	Dopamine	54	210	670
	Adrenaline	25	121	284
4	Caffeine	0	0	0
	Barbitone	0	0	0
	Riboflavin	0	<5	20
	Oxammonium hydrochloride	0	<5	18

Operating potential, 0.65 V versus calomel electrode; carrier, phosphate buffer (0.1 M, pH 7.4); injection of 100 μl aqueous solution of H_2O_2 (10 μmol/L) containing the interferents.

Table 2
Results of H_2O_2 analysis in hair dye of certain brand

Hair dye samples	Concentration			Reference method
Times of the determination	Conc. (H_2O_2) in cell (μM)	Conc. (H_2O_2) in real samples (mM)[a]	R.S.D.[b]	$KMnO_4$ titration
6	2.6 μM	85.0 μg/g	3.2%	87.2 μg/g

[a] Conc. (H_2O_2) in real samples is obtained by multiplying the detected value by the dilution factor.
[b] R.S.D. is the relative standard deviation of the six measurements by the sensor.

is lower for the film containing insufficient MnO_2 nanoparticles, because the surface area is low. On the other hand, too much MnO_2 in the film decreases conductivity and slows mass transport through the film. If the ratio between MnO_2 and Na-montmorillonite is too high, the MnO_2 particles cannot be dispersed sufficiently and may agglomerate to larger particles with reduced surface area. Optimization of the ratio between MnO_2 and Na-montmorillonite is demonstrated in Fig. 4. It shows that the current increases quickly and then slightly decreases with increasing MnO_2 concentration. The optimal concentration of MnO_2 in the colloidal Na-montmorillonite dispersion is 5 mg mL^{-1}.

The amount of the dispersion on the GCE surface determines the thickness of the film, and therefore influences the amperometric response of H_2O_2. The current response increased gradually with increasing film thickness. However, when the amount of colloidal dispersion exceeds 5 μL, the film becomes too thick and blocks electron transfer. Therefore, the 5 μL colloidal dispersion was chosen.

The effect of solution pH on the amperometric response for 1 mM H_2O_2 in 0.1 M PB solution is examined in Fig. 5. The catalytic ability of the film increases with pH reaching a maximum at pH 6.8. In this work, pH = 7.4 (0.1 M PB buffer) was selected because we plan further work at physiological pH.

The relationship between the oxidation current and the concentration of H_2O_2 was examined in a PB solution (pH = 7.4). The solution was stirred to ensure uniform distribution of H_2O_2 in the cell. Fig. 6 displays the amperometric response for the H_2O_2. When the same amount of H_2O_2 (0.5 mM/addition) was injected into the cell, the current was recorded instantly. Calibration curves for H_2O_2 measurement are also presented in Fig. 6. The current is linear for concentrations of H_2O_2 from 5×10^{-7} to 7.5×10^{-3} M. The sensitivity of the sensor to H_2O_2 was calculated to be 3.14×10^{4} μA M^{-1} cm^{-2}. The detection limit was estimated to be 1.5×10^{-7} M (S/N = 3).

Compared with the electrode modified by Horseradish peroxidase (HRP) (Deng and Dong, 1994; Oungpipat et al., 1995; Razola et al., 2002; Lei et al., 2003, 2004), MnO_2/Na-montmorillonite film sensors do not lose activity with increasing time. If the sensor is used each day for 10 measurements and each measurement takes 1 h, ten days later 95% of the initial response of the sensor is retained.

Four groups of substances that potentially coexist with H_2O_2 were investigated for their interference on H_2O_2 (Table 1). Most anions (Group 1) such as nitrate, sulfate, chlorate, perchlorate, and ferricyanide do not interfere when present in 100-fold mass excess. Amino acids (Group 2) slightly reduce the signal of hydrogen peroxide if they are present at 50 times the concentration of H_2O_2. Probably H_2O_2 in the sample solution is consumed by redox processes. Substances that potentially exist in biological liquids (Group 3) interfere strongly. Ascorbic acid, uric acid, dopamine and adrenaline increase the amperometric responses markedly when their concentrations are 5 times the concentration of H_2O_2. This may be assigned to strong redox processes. However, in most cases, the species in food and drug do not interfere the signals of H_2O_2. Group 4 lists some of these species. They have little if any interference on the H_2O_2 measurements. Thus, this H_2O_2 sensor can be used for the determination of H_2O_2 in cosmetics, foods, and drugs except the presence of strong reducing biological molecules in high concentration.

Several commodities have been tested for the measurement of H_2O_2. Experimental results agree with the $KMnO_4$ titration method. Here we only list the results of the measurement of H_2O_2 in a sample of hair dye (Table 2). The sample was weighed and dissolved in water to certain volume immediately before analysis. Amperometric determinations were made by adding the sample solutions directly after adding with 0.2, 0.4 and 0.6 mM H_2O_2 as internal standards. The recovery of the experiments was from 94.93% to 105.47% for 3 parallel measurements. These results proved that the sensor could be used to measure the concentration of real samples.

4. Conclusions

A high sensitivity H_2O_2 sensor was constructed with MnO_2 nanoparticles and Na-montmorillonite. The high sensitivity of this H_2O_2 sensor is attributed to the high specific surface area of the MnO_2 nanoparticles and the property of Na-montmorillonite to form a uniform film. The Na-montmorillonite encages the nanoparticles while allowing H_2O_2 to penetrate through the film. Ease of preparation and long-term stability make these sensors superior to horseradish peroxidase modified sensors, which must be stored in buffer. Its applicability to practical samples was demonstrated by measuring H_2O_2 in hair dye. Its low detection limit and its applicability in neutral and slightly alkaline media suggest that the MnO_2/montmorillonite system can probably act as a useful electrode material for the development of sensors.

Acknowledgements

This work was supported by the National Natural Science Foundation of China (Nos. 30370397 and 60571042). The authors are grateful to Dr. Liangjie Yuan for providing nano-MnO_2 materials.

References

Boyer, A., Kalcher, K., Pietsch, R., 1990. Graphite paste electrodes. Effects of paste composition and surface states on electron-transfer rates. Electroanalysis 2, 155–161.

Cai, X., Kalcher, K., Kolbl, G., Neuhold, C., Diewald, W., Ogorevc, B., 1995. Electrocatalytical reduction of hydrogen peroxide on a palladium-modified carbon paste electrode. Electroanalysis 7, 340–345.

Chi, Q., Dong, S., 1995. Amperometric biosensors based on the immobilization of oxidases in a Prussian blue film by electrochemical codeposition. Anal. Chim. Acta 310, 429–436.

Cox, J.A., Jaworski, R.K., 1989. Voltammetric reduction and determination of hydrogen peroxide at an electrode modified with a film containing palladium and iridium. Anal. Chem. 61, 2176–2178.

Dekany, L., Turi, L., Tombacz, E., Fendler, J.H., 1995. Preparation of size quantized CdS and ZnS particles in nanophase reactors provided by binary liquids adsorbed at layered silicates. Langmuir 11, 2285–2292.

Deng, Q., Dong, S.J., 1994. Mediatorless hydrogen peroxide electrode based on horseradish peroxidase entrapped in poly(*o*-phenylenediamine). J. Electroanal. Chem. 337, 191–196.

Emir, T., Kalcher, K., Schachl, K., Komersova, A., Bartos, M., Moderegger, H., Svancara, I., Vytras, K., 2001. Amperometric determination of glucose with a MnO_2 and glucose oxidase bulk-modified screen-printed carbon ink biosensor. Anal. Lett. 34, 2633–2647.

Emir, T., Josef, K., Emira, K., Negussie, W.B., Helmut, M., Emin, S., Sabina, B., Kurt, K., 2005. Amperometric determination of bonded glucose with a MnO_2 and glucose oxidase bulk-modified screen-printed electrode using flow-injection analysis. Talanta 65, 559–564.

Enea, O., Bard, A.J., 1986. Photoredox reactions at semiconductor particles incorporated into clays. CdS and ZnS+CdS mixtures in colloidal montmorillonite suspensions. J. Phys. Chem. 90, 301–306.

Fitch, A., Du, J., 1991. Diffusion layer in well-ordered clay-modified electrodes. J. Electroanal. Chem. 319, 409–414.

Fitch, A., Du, J., 1993. Effect of clay charge on $Cr(bpy)_3^{3+}$ reaction mechanism at clay-modified electrodes. J. Electroanal. Chem. 344, 45–59.

Fitch, A., Du, J., 1995. Computerized system for dual electrode multi-sweep cyclic voltammetry: its use in clay-modified electrode studies. Anal. Chem. 67, 1322–1325.

Gao, Z., Ivaska, A., Li, P., Lui, K., Yang, J., 1992. Electrocatalysis and flow-injection analysis of hydrogen peroxide at a chemically modified electrode. Anal. Chim. Acta 259, 211–218.

Itaya, K., Shoji, N., Uchida, I., 1984. Catalysis of the reduction of molecular oxygen to water at Prussian Blue modified electrode. J. Am. Chem. Soc. 106, 3423–3429.

Joo, P., Fitch, A., Mellican, S., Macha, S., 1996. Inorganic semiconductor nanoparticles and organic semiconductor nanowires in clay-minerals: electrochemical and fiber optic survey. NATO ASI Series, Series 3: High Technology, Nanoparticles in Solids and Solutions, vol. 18, pp. 529–541.

Kamat, P.V., 1984. Electrochemistry and photoelectrochemistry of dye-incorporated clay-modified electrode. J. Electroanal. Chem. 163, 389–394.

Karyakin, A.A., Gitelmacher, O.V., Karyakina, E.E., 1995. Prussian Blue-based first-generation biosensor. A sensitive amperometric electrode for glucose. Anal. Chem. 67, 2419–2423.

Karyakin, A.A., Karyakina, E.E., Gorton, L., 1996. Prussian-Blue-based amperometric biosensors in flow-injection analysis. Talanta 43, 1597–1606.

Karyakin, A.A., Karyakina, E.E., Gorton, L., 1999. On the mechanism of H_2O_2 reduction at Prussian Blue modified electrodes. J. Electrochem. Commun. 1, 78–82.

Karyakin, A.A., Karyakina, E.E., Gorton, L., 2000. Amperometric biosensor for glutamate using Prussian Blue-based “artificial peroxidase” as a transducer for hydrogen peroxide. Anal. Chem. 72, 1720–1723.

Klemens, S., Hailemichael, A., Kurt, K., Jitka, J., Ivan, S., Karel, V., 1997. Amperometric determination of hydrogen peroxide with a manganese dioxide-modified carbon paste electrode using flow injection analysis. Analyst 122, 985–989.

Kotov, N., Fendler, J. H., Tombacz, E., Dekany, I., 1992. CdS particles in organoclay complexes. Proc. — Conf. Colloid Chem., 6th (1993), 254–7.

Kurian, M., Galvin, M.E., Trapa, P.E., Sadoway, D.R., Mayes, A.M., 2005. Single-ion conducting polymer-silicate nanocomposite electrolytes for lithium battery applications. Electrochim. Acta 50 (10), 2125–2134.

Lei, C., Hu, S., Shen, G., Yu, R., 2003. Immobilization of horseradish peroxidase to a nano-Au monolayer modified chitosan-entrapped carbon paste electrode for the detection of hydrogen peroxide. Talanta 59, 981–988.

Lei, C., Wang, H., Shen, Yu.R., 2004. Immobilization of enzymes on the nano-Au film modified glassy carbon electrode for the determination of hydrogen peroxide and glucose. Electroanalysis 16, 736–740.

Mannino, S., Cosino, M.S., Ratti, S., 1993. Cobalt(II, III)-oxide chemically modified electrode as amperometric detector in flow injection systems. Electroanalysis 5, 145–148.

Oungpipat, W., Alexander, P., Southwell-Kelly, P., 1995. A reagentless amperometric biosensor for hydrogen peroxide determination based on asparagus tissue and ferrocene mediation. Anal. Chim. Acta 309, 35–45.

Oyama, N., Anson, F.C., 1986. Catalysis of the electroreduction of hydrogen peroxide by montmorillonite clay coatings on graphite electrode. J. Electroanal. Chem. 199, 467–470.

Pinnavaia, T.J., 1983. Intercalated clay catalysts. Science 220, 365–371.

Razola, S.S., Ruiz, B.L., Diez, N.M., Mark Jr., H.B., Kauffmann, J.M., 2002. Hydrogen peroxide sensitive amperometric biosensor based on horseradish peroxidase entrapped in a polypyrrole electrode. Biosens. Bioelectron. 17, 921–928.

Rice, M.E., Galus, Z., Adams, R.M., 1983. Graphite paste electrodes effects of paste composition and surface states on electron-transfer rates. J. Electroanal. Chem. 143, 89–102.

Samo, B.H., Bozidar, O., Klemens, S., Kurt, K., 2004. Glucose microbiosensor based on MnO_2 and glucose oxidase modified carbon fiber microelectrode. Electroanalysis 16, 1711–1716.

Song, X., Qiu, G., Qu, P., Yang, Z., 2005. Dispersion behavior of CeO_2 nanoparticles in water suspension. Xiyou Jinshu 29 (2), 167–172.

Taha, Z., Wang, J., 1991. Electrocatalysis and flow detection at a glassy carbon electrode modified with a thin film of oxymanganese species. Electroanalysis 3, 215–219.

Van Olphen, H., 1977. An Introduction to Clay Colloid Chemistry, 2nd Ed. John Wiley & Sons, Inc., New York.

Wang, J., Naser, N., Angnes, L., Wu, H., Chen, L., 1992. Metal-dispersed carbon paste electrode. Anal. Chem. 64, 1285–1288.

Yao, S., Xu, J., Wang, Y., Chen, X., Xu, Y., Hu, S., 2006. A high sensitive hydrogen peroxide amperometric sensor based on MnO_2 nanoparticles and dihexadecyl hydrogen phosphate composite film. Anal. Chim. Acta 557 (1–2), 78–84.

Yin, L., Chou, J., Chung, W., Sun, T., Hsiung, K., Hsiung, S., 2001. Glucose ENFET doped with MnO_2 power. Sens. Actuators, B, Chem. 76, 187–192.

Yoneyama, H., Haga, S., Yamanaka, S., 1989. Photocatalytic activities of microcrystalline TiO_2 incorporated in sheet silicates of clay. J. Phys. Chem. 93, 4833–4837.

Yuan, L., Li, Z., Sun, J., Zhang, K., Zhou, Y., 2003. Synthesis and characterization of activated MnO_2. Mater. Lett. 57, 1945–1948.